PHYSICAL REVIEW D **92,** 034001 (2015)

Glueballs from the Bethe-Salpeter equation

Helios Sanchis-Alepuz,[1] Christian S. Fischer,[1] Christian Kellermann,[2] and Lorenz von Smekal[2]
[1]*Institut für Theoretische Physik, Justus-Liebig-Universität Gießen, Heinrich-Buff-Ring 16, 35392 Gieß en, Germany*
[2]*Institut für Kernphysik, TU Darmstadt, Theoriezentrum, Schlossgartenstraße 2, 64289 Darmstadt, Germany*
(Received 17 April 2015; published 3 August 2015)

We formulate a framework to determine the mass of glueball states of the Landau gauge Yang-Mills theory in the continuum. To this end we derive a Bethe-Salpeter equation for two gluon bound states including the effects of Faddeev-Popov ghosts. We construct a suitable approximation scheme such that the interactions in the bound state equation match a corresponding successful approximation of the Dyson-Schwinger equations for the Landau gauge ghost and gluon propagators. Based upon a recently obtained solution for the propagators in the complex momentum plane we obtain results for the mass of the 0^{++} and 0^{-+} glueballs. In the scalar channel we find a mass value in agreement with lattice gauge theory.

DOI: 10.1103/PhysRevD.92.034001 PACS numbers: 12.38.Lg, 12.38.-t, 12.38.Aw

I. INTRODUCTION

The "physical" spectrum of pure Yang-Mills theory is made out of glueballs [1]. There is substantial evidence, both from lattice calculations (see [2,3] and references therein) and results from Dyson-Schwinger equations (DSEs) for the Landau gauge gluon propagator [4–6] that transverse gluons violate positivity and therefore cannot be part of the asymptotic state space of the theory. Consequently, the first physical excitation of the Yang-Mills vacuum is the lowest lying glueball state.

It is an important task to determine the mass of this state. Indeed, the properties of glueballs have been investigated since their prediction in the middle of the 1970s [1]. Today, the glueball masses in pure Yang-Mills theory are known rather accurately owing to high statistics lattice calculations [7–9]. Unquenched lattice calculations are also available, although there are considerable uncertainties in the determination of unquenched glueball masses [10–14]. This is mainly due to severe problems with the signal to noise ratio, thus requiring large statistics. In principle, it is also not easy to disentangle states with large glueball components from states dominated by other constituents such as quark-antiquark pairs. Naturally, this problem has a counterpart in the experiments: a glueball cannot be distinguished from a meson by quantum numbers and masses only. The determination of the decay channels of a given state is therefore vital for its identification. Ongoing and new experiments such as BES III [15] and PANDA [16] have dedicated parts of their programs to the identification of heavy glueballs in the charmonium region and beyond.

Alternative theoretical frameworks such as Hamiltonian many body [17–20] and strong coupling methods [21], potential approaches [22], Wilson loop based calculations [23], flux tube models [24], chiral Lagrangians [25–27], light front quantization [28] and the AdS/QCD approach [29] have shed some light on potential mass patterns and identifications of experimental states dominated by their glueball content. However, it seems fair to state that a detailed understanding of glueball formation from the underlying dynamics of Yang-Mills theory is still missing. In this paper we report on further steps toward such an understanding.

Working in Landau gauge, we construct homogeneous Bethe-Salpeter equations (BSEs) for glueballs which take into account the dynamics of gluon and ghost propagation as well as their interactions with one another. This is detailed in Secs. II and III, where we also discuss the general form of Bethe-Salpeter vertices for any quantum number. The calculation is performed in Euclidean space, which implies that the bound-state constituents are probed for complex momenta. In the literature, exploratory BSE calculations using instantaneous approximations [30] or extrapolations of the propagators into the complex momentum plane [31] can be found. In this work we present first results for self-consistent and covariant BSE calculation of glueballs in Landau gauge using explicit solutions for the ghost and gluon propagator DSEs in the complex momentum plane [6]. These are summarized in Sec. IV.

II. BOUND STATE EQUATIONS FOR GLUEBALLS

Our goal in this section is to provide a Bethe-Salpeter equation describing a glueball made from two gluons that are solutions of the DSE for the gluon propagator. A similar concept has proven very successful in the context of mesons, where the BSE of a quark-antiquark pair is used in connection with the corresponding DSE for the quark propagator, see e.g. [32–34] for reviews. A key property of this framework is consistency of the approximations made in the DSE and BSE. For mesons this implies to satisfy an axial Ward-Takahashi identity thus implementing constraints due to chiral symmetry and its breaking. One way of devising such a truncation is to derive both the

truncation of the DSE and the truncation of the BSE on common grounds using a two particle irreducible effective action (2PIEA). In the following we work along this strategy. Since we are working in Landau gauge we need to take into account the Faddeev-Popov ghosts. Thus we need a generalization of the usual BSE scheme that allows for mixing of bound states of different fields. In the following we will give a derivation of a suitable set of bound state equations that provide the necessary couplings of bound state amplitudes with different field content [35].

We consider the following 2PIEA,

$$\Gamma[D,G] = \frac{1}{2}\mathrm{Tr}\ln D_0 D^{-1} + \frac{1}{2}\mathrm{Tr} D_0^{-1} D - \mathrm{Tr}\ln G_0 G^{-1} - \mathrm{Tr} G_0^{-1} G + \Gamma_2[D,G], \quad (1)$$

where D and G are the gluon and ghost propagators. The interaction term is given diagrammatically by

$\Gamma_2[D,G] =$ 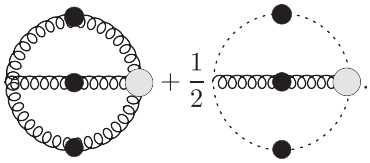 (2)

Each term contains one bare and one dressed vertex, the latter being represented by the shaded circles. The 2PIEA is already truncated, i.e. we have left out all diagrams including the four-gluon interaction. Furthermore, the dressed ghost-gluon and three-gluon vertices are assumed to be represented by suitable explicit expressions that capture the essence of the nonperturbative interactions. Such Ansatze have been employed successfully in the past [33]; we come back to this point in Sec. IV.

The corresponding Dyson-Schwinger equations for the ghost- and gluon propagators can be found by variation of the effective action with respect to a propagator, i.e.

$$\frac{\delta\Gamma[D,G]}{\delta D} = -D^{-1} + D_0^{-1} + \Sigma_D[D,G] = 0 \quad (3)$$

$$\frac{\delta\Gamma[D,G]}{\delta G} = 2G^{-1} - 2G_0^{-1} + \Sigma_G[D,G] = 0, \quad (4)$$

where we have $\Sigma_A = \frac{\delta\Gamma_2}{\delta A}$ with $A \in \{D,G\}$. Diagrammatically, the resulting DSEs read

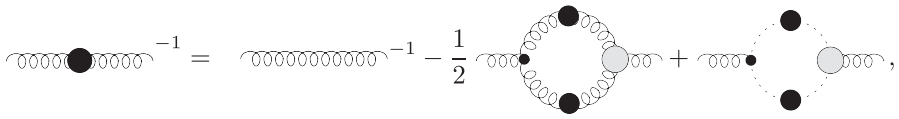 (5)

 (6)

We now proceed along the lines of Ref. [35]. In the following we will use a shorthand notation omitting the space-time arguments and indicating primed arguments by primed functions. We denote the solutions of DSEs (3) and (4) by $\hat{D}$ and $\hat{G}$ and perform a variation in two variables. Keeping only the linear terms we arrive at

$$\left.\frac{\delta\Gamma[D,G]}{\delta D}\right|_{\hat{D}+\delta_D,\hat{G}+\delta_G} \approx \left.\frac{\delta\Gamma[D,G]}{\delta D}\right|_{\hat{D},\hat{G}} + \int d^4x' d^4y' \left.\frac{\delta^2\Gamma[D,G]}{\delta D\delta D'}\right|_{\hat{D},\hat{G}} \delta'_D + \int d^4x' d^4y' \left.\frac{\delta^2\Gamma[D,G]}{\delta D\delta G'}\right|_{\hat{D},\hat{G}} \delta'_G \quad (7)$$

$$\left.\frac{\delta\Gamma[D,G]}{\delta G}\right|_{\hat{D}+\delta_D,\hat{G}+\delta_G} \approx \left.\frac{\delta\Gamma[D,G]}{\delta G}\right|_{\hat{D},\hat{G}} + \int d^4x' d^4y' \left.\frac{\delta^2\Gamma[D,G]}{\delta G\delta D'}\right|_{\hat{D},\hat{G}} \delta'_D + \int d^4x' d^4y' \left.\frac{\delta^2\Gamma[D,G]}{\delta G\delta G'}\right|_{\hat{D},\hat{G}} \delta'_G. \quad (8)$$

Using again the equations of motion we require for the solutions $\hat{D}$ and $\hat{G}$ to be stable that

$$\int d^4x' d^4y' \left.\frac{\delta^2\Gamma[D,G]}{\delta D\delta D'}\right|_{\hat{D},\hat{G}} \delta'_D + \left.\frac{\delta^2\Gamma[D,G]}{\delta D\delta G'}\right|_{\hat{D},\hat{G}} \delta'_G = 0 \quad (9)$$

and

$$\int d^4x' d^4y' \left.\frac{\delta^2\Gamma[D,G]}{\delta G\delta D'}\right|_{\hat{D},\hat{G}} \delta'_D + \left.\frac{\delta^2\Gamma[D,G]}{\delta G\delta G'}\right|_{\hat{D},\hat{G}} \delta'_G = 0. \quad (10)$$

Diagrammatically, the scattering kernels of the BSEs can be obtained by cutting a further line in the self-energy diagrams with respect to the desired second constituent in the bound state. The variations δ'_D, δ'_G are identified with the Bethe-Salpeter vertices χ_D and χ_G.

We then find the following coupled system of BSEs for ghost and gluon bound states

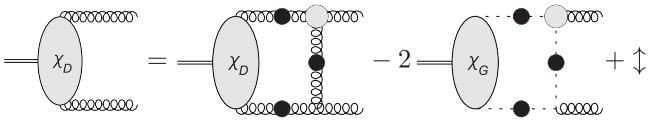

(11)

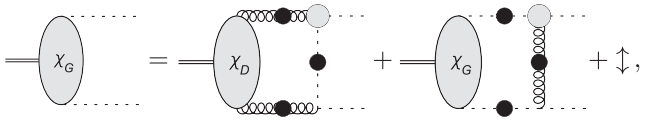

(12)

where the arrow indicates symmetrization of the kernels with respect to the dressed vertices. The resulting coupled system of two-body equations serves to describe glueballs as bound states of either a gluon or a ghost-antighost pair. The latter is necessary in the Landau gauge and represents contributions from the Faddeev-Popov determinant to the glueball masses. We will later discuss the relative importance of both contributions in different channels. For now we just emphasize that neither the ghosts nor the gluons are physical constituents in the sense that they do not appear as propagating particles in the positive definite part of the asymptotic state space of QCD [4–6]. Note, that there is no mixed gluon-ghost (or gluon-antighost) contribution to the glueball vertex. Such gluon-(anti)ghost bound states, if existent, may be members of a Becchi-Rouet-Stora-Tyutin quartet together with transverse gluons and, thus, part of the unphysical Hilbert space [36].

The above system of BSEs within Yang-Mills theory can be further generalized to full QCD by including quark contributions. Considering the corresponding effective action

$$\begin{aligned}\Gamma[D,G,S] = &\frac{1}{2}\mathrm{Tr}\ln D_0 D^{-1} + \frac{1}{2}\mathrm{Tr}D_0^{-1}D - \mathrm{Tr}\ln G_0 G^{-1} \\ &- \mathrm{Tr}G_0^{-1}G - \mathrm{Tr}\ln S_0 S^{-1} - \mathrm{Tr}S_0^{-1}S \\ &+ \Gamma_2[D,G,S],\end{aligned} \tag{13}$$

with diagrammatic representation

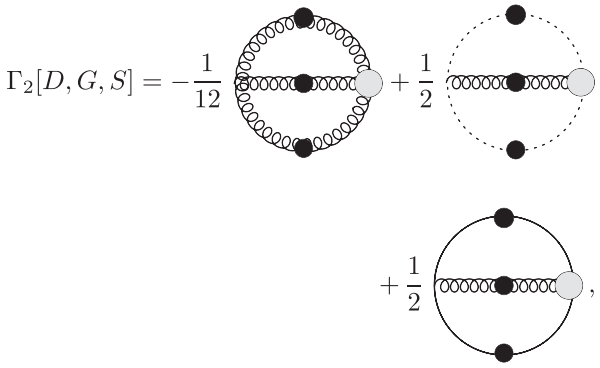

(14)

we can apply the same derivation as before considering variations with respect to all types of propagators. We then find the full system of coupled bound state two-body equations

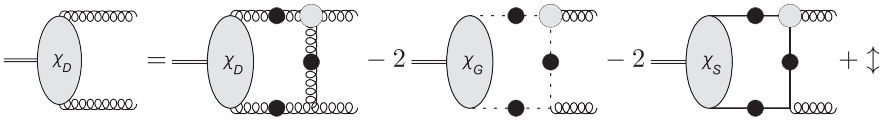

(15)

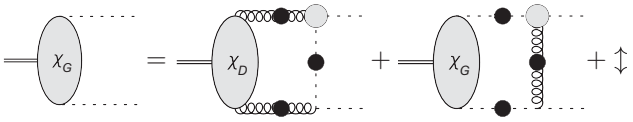

(16)

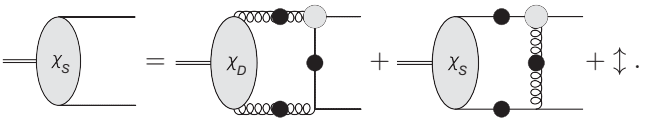

(17)

This set of BSEs describes mesons and glueballs in an approximation that can be seen as a generalized ladder truncation. Note, that the last diagram in (15) and the first of (17) provide for glueball/meson mixing. Although in this work we will restrict our explicit calculations to pure Yang-Mils theory we would like to add some comments on the influence of these terms onto the flavor singlet meson spectra.

In the pseudoscalar channel these terms generate a contribution to η–η' splitting. In the framework of BSEs the conventional approach to this problem is to include beyond rainbow-ladder terms connected with the axial anomaly in the quark-gluon interaction [37–39]. Our framework provides the additional effect of a direct mixing of the flavor-singlet η_0-meson with the $J^{PC} = 0^{-+}$ pseudoscalar glueball. Both effects together affect the η_0-meson mass. Our set of BSEs provides the simplest means of consistently including such glueball/meson mixing into BSE calculations. However, since in lattice calculations the mass of the pure glue pseudoscalar glueball is found to be around 2.5 GeV [9], it is not clear how large these mixing effects might be.

Considerable mixing effects may be expected, however, in the scalar meson sector, where there seem to be more states than one can accommodate in conventional quark antiquark multiplets [40]. While some of these states can well be accounted for by large four-quark components [41–43], others may very well be characterized by a dominant glueball contribution. The set of equations (15) to (17) may well provide a viable starting point for sophisticated investigations of a realistic scalar meson spectrum.

Finally, we need to comment on the number of constituents needed in our framework. In general, in a Bethe-Salpeter framework it is sufficient to explicitly account for only a minimal set of constituents that is necessary to carry the quantum numbers of the object in question. For (nonexotic) mesons this is guaranteed by a quark-antiquark pair. If there is a bound state it will appear in this equation with the correct mass. In addition, one has to keep in mind that a meson calculated in such a scheme also contains an infinite amount of additional gluons and quark-antiquark pairs simply due to the fully dressed nature of the internal propagators of the (valence) quark-antiquark pair. In the glueball sector, two constituent gluons are sufficient to account for the quantum numbers of glueballs with charge conjugation $\mathrm{C} = +1$. However, three gluons are the minimal set necessary to account for the charge conjugation odd states $\mathrm{C} = -1$. Thus, these cannot be described in our current framework. On the other hand, it is not necessary to account for four or even n valence gluons, since bound states will already appear in the two- and three-gluon equations.

In the following, we will focus on the coupled system of bound states for a pure gauge theory neglecting quarks [Eqs. (11) and (12)]. To solve this system numerically, we need reliable information on the nonperturbative propagaors of ghosts and gluons as well as a general expression for the bound state vertices χ_D and χ_G. In the next section we will discuss the latter, providing suitable expressions for arbitrary quantum numbers of glueballs.

III. BOUND STATE VERTICES FOR GLUEBALLS

We will now show how suitable bound state vertices χ_D and χ_G to be used in Eqs. (11) and (12) can be constructed. We start our present discussion from some general observations.

A bound state of two relativistic particles can be described by three quantum numbers: total spin J, parity P and charge parity C. Furthermore there are only two characteristic momenta involved, conveniently chosen to be the total momentum t_μ and the relative momentum r_μ. These two vectors can be used to construct suitable vertices χ_D and χ_G for our bound state problem. The idea is to construct basic invariant vertices with correct parity and charge conjugation properties and supplement these with an appropriate tensor representing a given total spin.

Let us first consider the vertex χ_D for the two-gluon bound state. A general scalar bound state vertex has to transform like a symmetric rank two Lorentz tensor for gluonic constituents. Thus it has to satisfy

$$\Lambda^\kappa{}_\mu \Lambda^\lambda{}_\nu T_{\kappa\lambda}(t, r) = T_{\mu\nu}(\Lambda t, \Lambda r). \tag{18}$$

The two simplest tensor structures with $J = 0$ that satisfy (18) are the metric tensor and a combination of the totally antisymmetric tensor and characteristic momenta:

$$\Gamma^{0^{++}}_{\mu\nu} = g_{\mu\nu}, \qquad \Gamma^{0^{-+}}_{\mu\nu} = \epsilon_{\kappa\lambda\mu\nu} r_\kappa t_\lambda. \tag{19}$$

The first structure represents a parity-even state. In general, there are three more symmetric and parity even structures that can be built from the total and relative momenta of the two gluons. Transversality in Landau gauge then restricts the total number of tensor components to two, see e.g. [17]. In our numerical studies we found that restricting to $g_{\mu\nu}$ already provides a very good approximation of the complete result using both structures. In contrast, the parity odd second structure in Eq. (19) is unique.

For the vertex χ_G composed of ghost fields the situation is trivial, since we are looking for a term that couples to scalars and transforms like a scalar itself. The appropriate vertex is the identity in Lorentz space and has positive parity. This restricted choice has interesting implications as discussed below.

In addition to the basic tensors in Eq. (19), representing the Lorentz structure of the constituents, we need suitable tensors representing a given total momentum J of the bound state. A Lorentz tensor representing a massive field with total spin J is required to have precisely $2J + 1$ independent components to represent the possible spin polarizations. The construction of such tensors is known and a detailed treatment can be found e.g. in [44]. We will repeat parts of the construction here in a slightly more explicit form focused directly on the construction of Bethe-Salpeter vertices. Consider first tensors $T_{a_1,\ldots,a_J}$ in three-space of rank J. To represent angular momentum J we require the tensor to be symmetric in all indices $T_{a_1\ldots a_J} = T_{\mathcal{P}[a_1\ldots a_J]}$ and traceless with respect to any pair of indices $\sum_m T_{\ldots m\ldots m\ldots} = 0$. The first constraint leaves the tensor

with $\frac{1}{2}(J^2+3J+2)$ independent components, while the second one imposes $\frac{1}{2}(J^2-J)$ further restrictions, thus leading to a tensor with $2J+1$ independent components, as required.[1] The construction of tensors in three-space is now easily transferred to four-tensors. If we require the tensor $T_{\mu_1\ldots\mu_J}$ to be transverse to the total momentum of the particle in every index $t^\nu T_{\ldots\nu\ldots}=0$ and adopt the particles rest-frame, we see that all components with timelike indices vanish, leaving only components with spacelike indices. So we are left with nothing else but the three-tensor considered before, which has $2J+1$ independent components. Thus we find the constraints for a Lorentz-tensor $T^J_{\mu_1\ldots\mu_J}$ of rank J to represent angular momentum J:

(1) T is symmetric in all indices,

$$T^J_{\mu_1\ldots\mu_J}=T^J_{\mathcal{P}[\mu_1\ldots\mu_J]}. \tag{20}$$

(2) T is transverse to the total momentum of the particle in every index,

$$t^\nu T^J_{\ldots\nu\ldots}=0. \tag{21}$$

(3) T is traceless in every pair of indices in the rest-frame,

$$T^{J,\ldots\lambda\ldots}_{\ldots\lambda\ldots}=0. \tag{22}$$

For the glueball masses we only need one such tensor from each multiplet. To construct such a tensor for angular momentum J one can build the J-fold tensor product of a transverse projector that transforms like a vector and then subtract the traces with respect to every pair of indices. Starting with $J=1$, a suitable transverse four-vector can be obtained by contracting the transverse projector $\tau_{\mu\nu}$ (with respect to the total momentum t) and the relative momentum r,

$$Q_\mu=\tau_{\mu\nu}r^\nu=\left(g_{\mu\nu}-\frac{t_\mu t_\nu}{t^2}\right)r^\nu=\left(r_\mu-\frac{(r\cdot t)t_\mu}{t^2}\right). \tag{23}$$

With only one Lorentz index this transverse vector already gives a possible angular momentum tensor for $J=1$. For higher J one builds symmetric J-fold tensor products of (23) by

$$\tilde{Q}_{\mu_1\ldots\mu_J}=Q_{\mu_1}\times\cdots\times Q_{\mu_J}. \tag{24}$$

The next step is to remove the traces of these tensors with respect to every pair of indices. This can be achieved with the general formula

$$\begin{aligned}T_{\mu_1\ldots\mu_J}=&\tilde{Q}_{\mu_1\ldots\mu_J}-(2J-1)^{-1}\sum_{P_{\mu_k}}\tau_{\mu_1\mu_2}\tilde{Q}^{\kappa}{}_{\kappa\mu_3\ldots\mu_J}\\&+(2J-1)^{-1}(2J-3)^{-1}\sum_{P_{\mu_k}}\tau_{\mu_1\mu_2}\tau_{\mu_3\mu_4}\tilde{Q}^{\kappa\lambda}{}_{\kappa\lambda\mu_5\ldots\mu_J}\\&-\cdots,\end{aligned} \tag{25}$$

where $\sum_P$ denotes the sum over all essentially different permutations of the indices.[2] We furthermore define

$$f_2=r^2-\frac{(r\cdot t)^2}{t^2}, \tag{26}$$

and the tensors[3]

$$B^{J,j}_{\mu_1\ldots\mu_J}=f_2^j\delta_{\{\mu_1\mu_2}\ldots\delta_{\mu_{2j-1}\mu_{2j}}\tilde{Q}^{(J-2j)}_{\mu_{2j+1}\ldots\mu_J\}},\qquad 2j<J, \tag{27}$$

$$B^{J,j}_{\mu_1\ldots\mu_J}=f_2^{J/2}\delta_{\{\mu_1\mu_2}\ldots\delta_{\mu_{J-1}\mu_J\}},\qquad 2j=J. \tag{28}$$

Using (25) and (24) together with the above definition, we finally obtain the desired total spin tensors in closed form as

$$T_{\mu_1\ldots\mu_J}=\tilde{Q}_{\mu_1\ldots\mu_J}+\sum_{j=1}^{2j\le J}(-1)^j\frac{1}{j!2^j}\left(\prod_{k=1}^{j}2(J-k)+1\right)^{-1}B^{J,j}_{\mu_1\ldots\mu_J}. \tag{29}$$

With these we have access to higher orbital angular momentum states built for glueballs with two gluon constituents (with $C=+1$) in the Lorentz singlet channels. For arbitrary even J we can use,

$$\Gamma^{J^{++}}_{\mu\nu,\mu_1\ldots\mu_J}(t^2,r^2,\theta)=T_{\mu_1\ldots\mu_J}A(t^2,r^2,\theta)g_{\mu\nu}, \tag{30}$$

$$\Gamma^{J^{-+}}_{\mu\nu,\mu_1\ldots\mu_J}(t^2,r^2,\theta)=T_{\mu_1\ldots\mu_J}A(t^2,r^2,\theta)(r\cdot t)r^\kappa t^\lambda\epsilon_{\kappa\lambda\mu\nu}, \tag{31}$$

and if J is odd,

$$\Gamma^{J^{++}}_{\mu\nu,\mu_1\ldots\mu_J}(t^2,r^2,\theta)=T_{\mu_1\ldots\mu_J}A(t^2,r^2,\theta)(r\cdot t)r^\kappa t^\lambda\epsilon_{\kappa\lambda\mu\nu}, \tag{32}$$

$$\Gamma^{J^{-+}}_{\mu\nu,\mu_1\ldots\mu_J}(t^2,r^2,\theta)=T_{\mu_1\ldots\mu_J}A(t^2,r^2,\theta)g_{\mu\nu}. \tag{33}$$

Here we have introduced scalar functions $A(t^2,r^2,\theta)$, which are even under inversion of the angle θ between r and t. The additional factors $(r\cdot t)$ ensure the correct behavior of the bound state vertices under charge parity transformations,

[1] It is also possible to construct tensors representing half-odd integer spin. Since we are dealing with Bethe-Salpeter equations of two particles in the same representation, so that the total angular momentum is integer, we will not consider this possibility here but instead refer the interested reader again to [44].

[2] This means that the sum has to be divided by appropriate combinatorial factors.

[3] For the convenience of the reader we have denoted the rank of the raw tensors as a superscript.

which result in a simple flip of the sign of the relative momentum r_μ in our framework.

The corresponding vertices for glueballs with a ghost antighost pair as constituents are constructed along the same lines. For arbitrary positive parity even J we can use

$$\Gamma^{J^{++}}_{\mu_1\ldots\mu_J}(t^2, r^2, \theta) = T_{\mu_1\ldots\mu_J} A(t^2, r^2, \theta), \tag{34}$$

and if J is odd the negative parity states are obtained from

$$\Gamma^{J^{-+}}_{\mu_1\ldots\mu_J}(t^2, r^2, \theta) = T_{\mu_1\ldots\mu_J} A(t^2, r^2, \theta). \tag{35}$$

Note that the parity P of the angular momentum tensors $T_{\mu_1\ldots\mu_J}$ is given by $P = (-1)^J$. Thus the parity of the even (odd) J tensors is positive (negative). Hence there are neither contributions from ghost antighost pairs to glueballs for even J and with quantum numbers J^{-+}, nor for odd J with J^{++}. For the gluonic vertices the natural parity of the total spin tensors can be supplemented by the odd parity basis element given in (19), thus changing the overall parity of the tensor representation. This is not possible for the ghost vertices. Consequently, we only find the restricted set (34) and (35) of possible quantum numbers for glueball states with ghost contributions.

Another potential restriction for the contribution of gluonic vertices to glueballs has been frequently discussed in the literature in the context of model building [45]: if the gluonic constituents were massless and on-shell, *Yang's theorem* [46] would restrict the number of allowed quantum numbers drastically. In our framework this constraint appears to be almost irrelevant. The nonperturbative gluonic constituents that appear in the BSE are neither on-shell nor massless. Instead they acquire a dynamically generated mass, as discussed in more detail in the next section.[4] Thus, gluonic contributions in Yang-forbidden channels may be suppressed but certainly not forbidden. These channels are the 1^{++} and all odd J^{-+}-channels. Since in the 1^{++}-channel ghost contributions are absent as well, the potentially suppressed gluonic contributions may lead to an "unnaturally" large glueball mass in this channel. This is indeed observed in lattice calculations [8,9]. In the odd J^{-+}-channels, however, ghost contributions are allowed. If the suppression of the gluonic contributions were strong, these states could be termed "ghostballs." We will study such states in future work.

In addition, there may be another basic vertices for the gluons in the spin 2 channel, traceless symmetric tensors. For example, Landau constructed one for QED with $J^{PC} = 2^{++}$ [47]. The explicit form of this basic $J = 2$ tensor with our notations would read

$$\begin{aligned}\Gamma^{2^{++}}_{\mu\nu;\mu_1\mu_2} = {} & t^4\left(-\frac{1}{3}g_{\mu\nu}g_{\mu_1\mu_2} + \frac{1}{2}g_{\mu\mu_1}g_{\nu\mu_2} + \frac{1}{2}g_{\mu\mu_2}g_{\nu\mu_1}\right) \\ & + t^2\left(\frac{1}{3}g_{\mu\nu}t_{\mu_1}t_{\mu_2} - \frac{1}{2}g_{\mu\mu_1}t_\nu t_{\mu_2} - \frac{1}{2}g_{\mu\mu_2}t_\nu t_{\mu_1}\right. \\ & \left. - \frac{1}{2}g_{\nu\mu_1}t_\mu t_{\mu_2} - \frac{1}{2}g_{\nu\mu_2}t_\mu t_{\mu_1} + \frac{1}{3}g_{\mu_1\mu_2}t_\mu t_\nu\right) \\ & + \frac{2}{3}t_\mu t_\nu t_{\mu_1} t_{\mu_2},\end{aligned} \tag{36}$$

where the pair (μ, ν) denotes the Lorentz indices of the gluon constituents and (μ_1, μ_2) the one of the bound state. With such a tensor vertices for a given set of quantum numbers J^{PC} can be constructed in a similar way as from the two singlet tensors in Eqs. (19).

Having discussed the derivation of the bound state equations we will use to describe glueballs and the form of the necessary bound state vertices, we will now turn to the numerical part of our investigation. We will find that it is necessary to solve the system of coupled DSEs of ghost and gluon fields for complex momenta in order to use the resulting propagators in our calculation of glueballs.

IV. THE YANG-MILLS SYSTEM IN THE COMPLEX PLANE

We solve the coupled system of bound state equations, (15) and (16) in pure Yang-Mills theory in Euclidean momentum space. In the rest frame of the glueball, its total momentum is then given by $(0, 0, 0, im_B)$ with m_B is the bound-state mass. Without loss of generality, the total momenta can be shared equally between the two constituents. Their momenta are then given by $r_\pm = (r \pm t)/2$, with relative momentum r between the constituents. It is then clear that the internal propagator lines in BSEs are given by solutions of the DSEs for complex momenta.

These can be obtained from the corresponding coupled set of Dyson-Schwinger equations. In Landau gauge the ghost propagator $D_G(p^2)$ and the gluon propagator $D_{\mu\nu}(p^2)$ are given by

$$D_{\mu\nu}(p^2) = \left(\delta_{\mu\nu} - \frac{p_\mu p_\nu}{p^2}\right)\frac{Z(p^2)}{p^2}, \tag{37}$$

$$D_G(p^2) = -\frac{G(p^2)}{p^2}, \tag{38}$$

where the diagonal color structure has been omitted for brevity. Note that the gluon is transverse also nonperturbatively, thus spurious glueball states due to longitudinal modes, as present in some potential models [22], are

[4]Note that in the context of this discussion of Yang's theorem it is irrelevant whether the mass generation mechanism leads to an infrared vanishing gluon propagator ("scaling") or an infrared finite propagator ("decoupling"). Furthermore, "mass generation" in this context does not mean that the gluon propagator acquires a pole at timelike momenta, but merely that the zero-momentum pole of the free propagator disappears due to interactions.

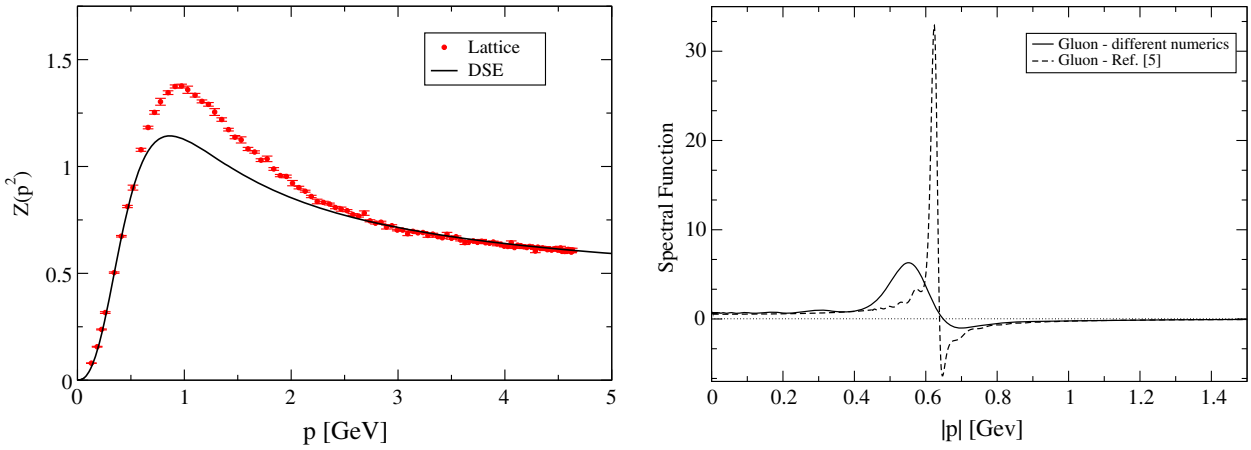

FIG. 1 (color online). Left: Results for the gluon dressing function $Z(p^2)$ from the DSEs [50] for real and spacelike momenta, compared with lattice calculations [60]. Right: Results for the gluon spectral function from DSEs for timelike momenta. Shown is the result from Ref. [6] together with result obtained in the same truncation scheme but with slightly different numerics, see main text for further explanations.

naturally avoided. The coupled system of DSE (omitting two-loop diagrams) has been displayed diagrammatically in Eqs. (5)–(6). This system of equations has been considered frequently in the past years. It has been solved analytically in the deep infrared, where exact solutions without any truncations are possible [48,49]. Two qualitatively different solutions have been found named "scaling" and "decoupling" [50,51]. Whereas the scaling solution consists of infrared power laws for all Green's functions with an infrared vanishing gluon propagator and an infrared divergent ghost, the decoupling solution is characterized by an infrared finite gluon propagator and a finite ghost dressing function. Current lattice calculations on large volumes clearly favor the decoupling type of solutions [52]; there is, however, an ongoing discussion on potentially significant effects from different gauge fixing strategies in the deep infrared [53–58]. In this work we concentrate on the decoupling type of solutions, which have been associated with a dynamically generated "gluon mass."[5] As already mentioned above, these still maintain transversality. At finite momenta, the equations have to be solved numerically and approximations for the dressed vertices need to be introduced. A suitable truncation scheme has been introduced in Ref. [59] and improved in Ref. [50]. It involves educated Ansatze for the ghost-gluon and three-gluon vertex and neglects the effects of the four-gluon interaction completely. The resulting modified system of equations has exactly the structure of the system (3) and (4) obtained from the variation of the 2PIEA (1) in Sec. II. For real momenta, we show the numerical solution for the gluon dressing function in Fig. 1. As can be seen from the comparison with the lattice results [60], there is very good agreement in the infrared and ultraviolet momentum region, whereas in the mid-momentum region one observes quantitative deviations. These deviations are certainly in part due to the neglected four-gluon interactions in the DSEs (5)–(6). They can be compensated, however, by suitably optimizing the input used for the dressed three-gluon vertex by simultaneously solving its own DSE together with those for the propagators [61].

The system of DSEs (5), (6) for the ghost and gluon propagator has been solved in the complex p^2 plane recently, see Ref. [6] for details. As explained above, this complex solution constitutes a vital input into the corresponding Bethe-Salpeter equation for the glueballs and is used in the following. In this respect it is important to note that the analytic structure of the gluon and ghost propagators as obtained in Ref. [6] shows branch cuts along the timelike momentum axis, i.e. for negative invariant momentum squared, but no singularities away from the real axis in the complex p^2 plane. For the real part of the gluon propagator this can be seen in Fig. 2, corresponding plots for the imaginary part and the ghost dressing function can be found in Ref. [6]. This behavior greatly helps in the numerical treatment of the BSE. Along the timelike axis of negative p^2 one can extract the gluon spectral function, which is shown in the right plot of Fig. 1. We have plotted the result from Ref. [6] together with a corresponding result obtained from an improved numerical method. The corresponding results are very similar except on a narrow region around the cut on the negative p^2-axis. As a result, one obtains a considerable smoother spectral function, as can be seen in Fig. 1. We use this improved result in the present work. At finite temperature, similar spectral functions were obtained using maximum entropy method reconstruction methods based on Euclidean results within the functional renormalization group framework [62].

[5]Of course, this "mass" is not to be identified with the mass of a physical particle. The analytic structure of the gluon propagator is clearly different from a simple mass pole [6].

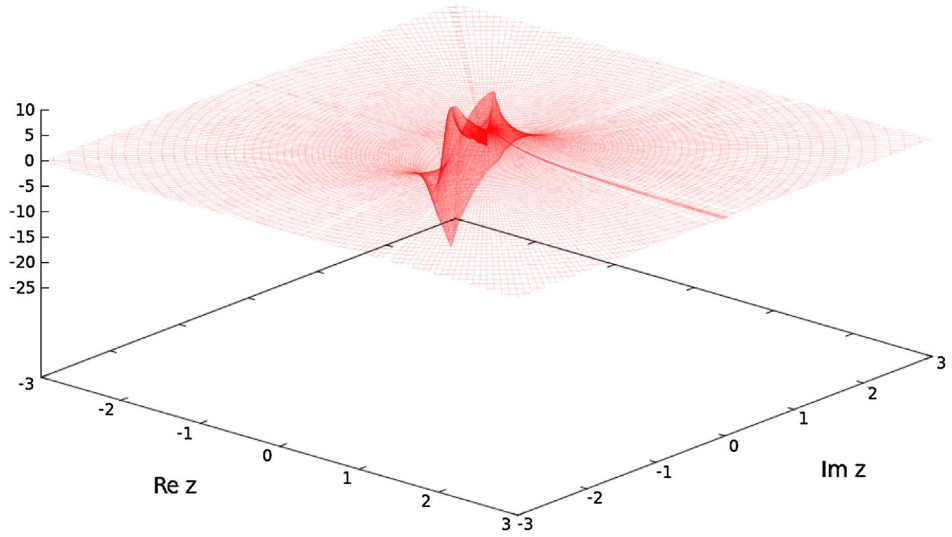

FIG. 2 (color online). Real part of the gluon propagator function $D(p^2) = Z(p^2)/p^2$ in the complex $z = p^2$ plane [6].

Finally, a comment on the scale is in order. This is fixed by comparison with the lattice results for the gluon propagator and remains fixed, i.e. it is not adjusted again in the glueball calculations. Thus, in principle, we obtain absolute values for the glueball masses.

V. LOWEST LYING GLUEBALL MASSES

We have solved the BSEs for a glueball in the scalar and pseudoscalar channel using the bound state equations (11) and (12) together with the vertices (30) to (33). For the propagators of ghosts and gluons we use the numerical results discussed in the last section.

Bound state vertices are not primitively divergent vertices and therefore they generically go to zero like power laws for large momenta [63]. In contrast to the behavior of meson BSEs, however, (11) and (12) also admit solutions with a logarithmic behavior in the UV. (Details on the asymptotic behavior of glueball BSEs together with an explicit analytic analysis will be given elsewhere.) These solutions do not correspond to bound states. In order to guide the iterative numerical procedure to the correct bound state solution it turns out to be sufficient to introduce an additional Pauli-Villars term into the purely gluonic diagram of (11) that depends on the momentum of the exchanged gluon propagator. Namely, we replace $Z(k^2) \to Z(k^2)(1 + k^2/\Lambda_{PV}^2)^{-1}$, with k^2 the momentum of the exchanged gluon and Λ_{PV} a cutoff scale. By inspection of the Bethe-Salpeter vertex functions we have verified, that such a term does not simply modify the logarithmic solutions of the BSE above the scale Λ_{PV}^2 but indeed drives the equation to a different and well-behaved solution. We find that the resulting glueball masses are insensitive to all values $\Lambda_{PV}^2 > 100$ GeV^2 of the scale that we have probed.

We present our results in Table I together with corresponding ones from lattice gauge theory, the Hamiltonian approach and Regge theory. Additionally, we compare to a rather recent calculation in a nonrelativistic constituent model.

Comparing with the lattice results, we find that the state with quantum numbers 0^{++} is well reproduced on the five percent level. Compared with the lattice, the good agreement of our result for the lowest lying scalar glueball is remarkable, though probably not surprising. As explained above, our truncation scheme for the ghost/gluon DSEs produces solutions which are pointwise similar to the lattice results in the low and high momentum region and display a twenty percent difference for momenta around 1 GeV. Thus the overall quality of the truncation scheme is well below the twenty percent range and thus in agreement with our findings for the scalar glueball mass. The remaining deficiencies in our truncation scheme are in the details of the three-gluon and the missing four-gluon interactions.

In contrast, the mass of the pseudoscalar glueball is much higher than that predicted by lattice calculations as well as by other approaches. As discussed in Sec. III there are no ghost contributions in these channels, leaving a greatly

TABLE I. Scalar and pseudoscalar glueball masses (in GeV) from various studies. We quote the Model B data from Ref. [22].

	Masses (GeV)			
J^{PC}	Lattice	Hamiltonian/ Regge theory	Constituent models	This work
0^{++}	1.71 (5)(8) [9]	1.98 [18]	1.71 [64]	1.64
	1.73 (5)(8) [8]	1.58 [23]	1.86 [22]	
0^{-+}	2.56 (4)(1) [9]	2.22 [18]	2.61 [64]	4.53
	2.59 (4)(13) [8]	2.56 [23]	2.49 [22]	

reduced BSE with only one gluonic diagram to be solved. This diagram is, in turn, largely dominated by the three-gluon vertex, both directly and via the solution of the DSE for the gluon propagator. Since the ansatz used here was devised in the context of the study of gluon and ghost DSEs for real momenta, it is conceivable that the behavior of this ansatz in the complex plane affects significantly the glueball spectrum in particular for states with no ghost-antighost content. The study of the connection between the details of the nonperturbative gluon self-interactions and their impact on glueball masses will be the subject of future work.

VI. SUMMARY

In this paper we have presented a framework that allows us to calculate glueball properties from the dynamics of Landau gauge Yang-Mills theory. We have constructed a set of bound state equations that includes both ghosts and gluons degrees of freedom thus taking into account also the effects of the Faddeev-Popov determinant. This set of equations allows for mixing of bound state contributions from different species of particles and is readily generalized to full QCD, including quarks. It thus naturally incorporates meson/glueball mixing. Furthermore we have presented suitable representations for the bound state vertices for arbitrary quantum numbers J^{PC}.

As an illustration of the framework, we have calculated the scalar and pseudoscalar glueball mass. Our result for the scalar glueball state is certainly encouraging, although in the pseudoscalar channel the mass is exceedingly high. Compared to the recent exploratory approach of Ref. [31] we have made a number of technical improvements. Most important are the use of explicit solutions of the ghost and gluon propagators in the complex momentum plane. Furthermore, our approach fully maintains multiplicative renormalizability.

Our framework for calculations of glueball properties offers various prospects of improvements and applications in the near future. First, different Ansatze for the three-gluon vertex should be used and its impact on the spectrum analyzed. It would be desirable, although technically very demanding, to use dynamical three-point vertices as in [61] and to include the four-gluon interaction contributions [65,66] into our framework. On the other hand, a very important extension is the inclusion of meson/glueball mixing along the lines of Eqs. (15) to (17). This will allow us to leave the sector of pure gauge field calculations of glueballs and thus provide access to realistic glueball properties in the future.

ACKNOWLEDGMENTS

We thank Gernot Eichmann and Richard Williams for helpful comments pointing out a misrepresentation in the original version of the manuscript. We also thank Reinhard Alkofer for fruitful discussions in the early stage of this work. This work was supported by the Helmholtz International Center for FAIR within the LOEWE program of the State of Hesse and by the BMBF Contract No. 06GI7121. H. S. A. has been supported by an Erwin Schroedinger fellowship J3392-N20 from the Austrian Science Fund, FWF.

[1] H. Fritzsch and P. Minkowski, Psi resonances, gluons and the Zweig rule, Nuovo Cimento Soc. Ital. Fis. **30A**, 393 (1975).
[2] P. O. Bowman, U. M. Heller, D. B. Leinweber, M. B. Parappilly, A. Sternbeck, L. von Smekal, A. G. Williams, and J.-b. Zhang, Scaling behavior and positivity violation of the gluon propagator in full QCD, Phys. Rev. D **76**, 094505 (2007).
[3] A. Maas, Describing gauge bosons at zero and finite temperature, Phys. Rep. **524**, 203 (2013).
[4] L. von Smekal, R. Alkofer, and A. Hauck, The Infrared Behavior of Gluon and Ghost Propagators in Landau Gauge QCD, Phys. Rev. Lett. **79**, 3591 (1997).
[5] R. Alkofer, W. Detmold, C. S. Fischer, and P. Maris, Analytic properties of the Landau gauge gluon and quark propagators, Phys. Rev. D **70**, 014014 (2004).
[6] S. Strauss, C. S. Fischer, and C. Kellermann, Analytic Structure of the Landau Gauge Gluon Propagator, Phys. Rev. Lett. **109**, 252001 (2012).
[7] G. S. Bali, K. Schilling, A. Hulsebos, A. C. Irving, C. Michael, and P. W. Stephenson (UKQCD Collaboration), A comprehensive lattice study of SU(3) glueballs, Phys. Lett. B **309**, 378 (1993).
[8] C. J. Morningstar and M. J. Peardon, The glueball spectrum from an anisotropic lattice study, Phys. Rev. D **60**, 034509 (1999).
[9] Y. Chen, A. Alexandru, S. J. Dong, T. Draper, I. Horvath, F. X. Lee, K. F. Liu, N. Mathur *et al.*, Glueball spectrum and matrix elements on anisotropic lattices, Phys. Rev. D **73**, 014516 (2006).
[10] A. Hart, and M. Teper (UKQCD Collaboration), On the glueball spectrum in O(a) improved lattice QCD, Phys. Rev. D **65**, 034502 (2002).
[11] G. S. Bali, B. Bolder, N. Eicker, T. Lippert, B. Orth, P. Ueberholz, K. Schilling, and T. Struckmann (TXL and T(X)L Collaborations), Static potentials and glueball masses from QCD simulations with Wilson sea quarks, Phys. Rev. D **62**, 054503 (2000).

[12] A. Hart, C. McNeile, C. Michael, and J. Pickavance (UKQCD Collaboration), A lattice study of the masses of singlet 0++ mesons, Phys. Rev. D **74**, 114504 (2006).
[13] C. M. Richards, A. C. Irving, E. B. Gregory, and C. McNeile (UKQCD Collaboration), Glueball mass measurements from improved staggered fermion simulations, Phys. Rev. D **82**, 034501 (2010).
[14] E. Gregory, A. Irving, B. Lucini, C. McNeile, A. Rago, C. Richards, and E. Rinaldi, Towards the glueball spectrum from unquenched lattice QCD, J. High Energy Phys. 10 (2012) 170.
[15] D. M. Asner, T. Barnes, J. M. Bian, I. I. Bigi, N. Brambilla, I. R. Boyko, V. Bytev, K. T. Chao *et al.*, Physics at BES-III, Int. J. Mod. Phys. A **24**, S1-794 (2009).
[16] M. F. M. Lutz *et al.* (PANDA Collaboration), Physics performance report for PANDA: Strong interaction studies with antiprotons, arXiv:0903.3905.
[17] A. Szczepaniak, E. S. Swanson, C.-R. Ji, and S. R. Cotanch, Glueball Spectroscopy in a Relativistic Many Body Approach to Hadron Structure, Phys. Rev. Lett. **76**, 2011 (1996).
[18] A. P. Szczepaniak and E. S. Swanson, The low lying glueball spectrum, Phys. Lett. B **577** (2003) 61.
[19] F. J. Llanes-Estrada, P. Bicudo, and S. R. Cotanch, Oddballs and a Low Odderon Intercept, Phys. Rev. Lett. **96**, 081601 (2006).
[20] P. Bicudo, S. R. Cotanch, F. J. Llanes-Estrada, and D. G. Robertson, The BES f0(1810): A new glueball candidate, Eur. Phys. J. C **52**, 363 (2007).
[21] H. P. Pavel, Expansion of the Yang-Mills Hamiltonian in spatial derivatives and glueball spectrum, Phys. Lett. B **685**, 353 (2010); SU(2) Dirac-Yang-Mills quantum mechanics of spatially constant quark and gluon fields, Phys. Lett. B **700**, 265 (2011).
[22] F. Brau and C. Semay, Semirelativistic potential model for glueball states, Phys. Rev. D **70**, 014017 (2004); V. Mathieu, C. Semay, and B. Silvestre-Brac, Semirelativistic potential model for three-gluon glueballs, Phys. Rev. D **77**, 094009 (2008).
[23] A. B. Kaidalov and Y. A. Simonov, Glueball masses and Pomeron trajectory in nonperturbative QCD approach, Phys. Lett. B **477**, 163 (2000).
[24] F. Buisseret, Meson and glueball spectra with the relativistic flux tube model, Phys. Rev. C **76**, 025206 (2007).
[25] S. He, M. Huang, and Q.-S. Yan, The pseudoscalar glueball in a chiral Lagrangian model with instanton effect, Phys. Rev. D **81**, 014003 (2010).
[26] S. Janowski, D. Parganlija, F. Giacosa, and D. H. Rischke, The glueball in a chiral linear sigma model with vector mesons, Phys. Rev. D **84**, 054007 (2011).
[27] W. I. Eshraim, S. Janowski, F. Giacosa, and D. H. Rischke, Decay of the pseudoscalar glueball into scalar and pseudoscalar mesons, Phys. Rev. D **87**, 054036 (2013).
[28] B. H. Allen and R. J. Perry, Glueballs in a Hamiltonian light front approach to pure glue QCD, Phys. Rev. D **62**, 025005 (2000); S. Dalley and B. van de Sande, Glueballs on a transverse lattice, Phys. Rev. D **62**, 014507 (2000).
[29] H. Boschi-Filho, N. R. F. Braga, F. Jugeau, and M. A. C. Torres, Anomalous dimensions and scalar glueball spectroscopy in AdS/QCD, Eur. Phys. J. C **73**, 2540 (2013).
[30] S. Rai Choudhury and A. N. Mitra, Glueballs under harmonic confinement, Phys. Rev. D **28**, 2201 (1983); J. Y. Cui, J. M. Wu, and H. Y. Jin, Glueball spectrum from the B.S. equation, Phys. Lett. B **424**, 381 (1998).
[31] J. Meyers and E. S. Swanson, Spin zero glueballs in the Bethe-Salpeter formalism, Phys. Rev. D **87**, 036009 (2013).
[32] P. Maris and C. D. Roberts, Dyson-Schwinger equations: A tool for hadron physics, Int. J. Mod. Phys. E **12**, 297 (2003).
[33] C. S. Fischer, Infrared properties of QCD from Dyson-Schwinger equations, J. Phys. G **32**, R253 (2006).
[34] A. Bashir, L. Chang, I. C. Cloet, B. El-Bennich, Y. X. Liu, C. D. Roberts, and P. C. Tandy, Collective perspective on advances in Dyson-Schwinger equation QCD, Commun. Theor. Phys. **58**, 79 (2012).
[35] R. Fukuda, Stability conditions in quantum system. A general formalism, Prog. Theor. Phys. **78**, 1487 (1987).
[36] N. Alkofer and R. Alkofer, Features of ghost-gluon and ghost-quark bound states related to BRST quartets, Phys. Lett. B **702**, 158 (2011).
[37] L. von Smekal, A. Mecke, and R. Alkofer, A dynamical eta-prime mass from an infrared enhanced gluon exchange, AIP Conf. Proc. **412**, 746 (1997).
[38] M. S. Bhagwat, L. Chang, Y.-X. Liu, C. D. Roberts, and P. C. Tandy, Flavour symmetry breaking and meson masses, Phys. Rev. C **76**, 045203 (2007).
[39] R. Alkofer, C. S. Fischer, and R. Williams, U(A)(1) anomaly and eta-prime mass from an infrared singular quark-gluon vertex, Eur. Phys. J. A **38**, 53 (2008).
[40] K. Nakamura *et al.* (Particle Data Group Collaboration), Review of particle physics, J. Phys. G **37**, 075021 (2010).
[41] R. L. Jaffe, Multi-quark hadrons. 1. The phenomenology of (2 quark 2 anti-quark) mesons, Phys. Rev. D **15**, 267 (1977).
[42] J. R. Pelaez, On the Nature of Light Scalar Mesons from their Large N(c) Behavior, Phys. Rev. Lett. **92**, 102001 (2004); J. R. Pelaez and G. Rios, Nature of the f0(600) from its N(c) Dependence at Two Loops in Unitarized Chiral Perturbation Theory, Phys. Rev. Lett. **97**, 242002 (2006).
[43] W. Heupel, G. Eichmann, and C. S. Fischer, Tetraquark bound states in a Bethe-Salpeter approach, Phys. Lett. B **718**, 545 (2012).
[44] C. Zemach, Use of angular momentum tensors, Phys. Rev. **140**, B97 (1965).
[45] T. Barnes, A transverse gluonium potential model with Breit-Fermi hyperfine effects, Z. Phys. C **10**, 275 (1981).
[46] C.-N. Yang, Selection rules for the dematerialization of a particle into two photons, Phys. Rev. **77**, 242 (1950); E. S. Swanson and A. P. Szczepaniak, Heavy hybrids with constituent gluons, Phys. Rev. D **59**, 014035 (1998); V. Mathieu, How many degrees of freedom has the gluon?, *Proc. Sci.*, QCD TNT09 (2009) 024 [arXiv:0910.4855].
[47] L. D. Landau, The moment of a 2-photon systemy, Dokl. Akad. Nauk **60**, 207 (1948).
[48] R. Alkofer, C. S. Fischer, and F. J. Llanes-Estrada, Vertex functions and infrared fixed point in Landau gauge SU(N) Yang-Mills theory, Phys. Lett. B **611**, 279 (2005); C. S. Fischer and J. M. Pawlowski, Uniqueness of infrared asymptotics in Landau gauge Yang-Mills theory, Phys. Rev. D **75**, 025012 (2007); Uniqueness of infrared asymptotics in Landau gauge Yang-Mills theory. II., Phys. Rev. D **80**, 025023 (2009).

[49] C. Lerche and L. von Smekal, On the infrared exponent for gluon and ghost propagation in Landau gauge QCD, Phys. Rev. D **65**, 125006 (2002); D. Zwanziger, Time-independent stochastic quantization, DS equations, and infrared critical exponents in QCD, Phys. Rev. D **67**, 105001 (2003); J. M. Pawlowski, D. F. Litim, S. Nedelko, and L. von Smekal, Infrared Behaviour and Fixed Points in Landau Gauge QCD, Phys. Rev. Lett. **93**, 152002 (2004).

[50] C. S. Fischer, A. Maas, and J. M. Pawlowski, On the infrared behavior of Landau gauge Yang-Mills theory, Ann. Phys. (Amsterdam) **324**, 2408 (2009).

[51] A. C. Aguilar, D. Binosi, and J. Papavassiliou, Gluon and ghost propagators in the Landau gauge: Deriving lattice results from Schwinger-Dyson equations, Phys. Rev. D **78**, 025010 (2008); Ph. Boucaud, J. P Leroy, A. Le Yaouanc, J. Micheli, O. Pène, and J. Rodríguez-Quintero IR finiteness of the ghost dressing function from numerical resolution of the ghost SD equation, J. High Energy Phys. 06 (2008) 012; On the IR behaviour of the Landau-gauge ghost propagator, J. High Energy Phys. 06 (2008) 099; D. Dudal, J. A. Gracey, S. P. Sorella, N. Vandersickel, and H. Verschelde, A refinement of the Gribov-Zwanziger approach in the Landau gauge: Infrared propagators in harmony with the lattice results, Phys. Rev. D **78**, 065047 (2008).

[52] A. Cucchieri and T. Mendes, Constraints on the IR behavior of the ghost propagator in Yang-Mills theories, Phys. Rev. D **78**, 094503 (2008); Constraints on the IR Behavior of the Gluon Propagator in Yang-Mills Theories, Phys. Rev. Lett. **100**, 241601 (2008); Lattice gluodynamics computation of Landau gauge Green's functions in the deep infrared, Phys. Lett. B **676**, 69 (2009).

[53] L. von Smekal, Landau gauge QCD: Functional methods versus lattice simulations, arXiv:0812.0654.

[54] A. Sternbeck and L. von Smekal, Infrared exponents and the strong-coupling limit in lattice Landau gauge, Eur. Phys. J. C **68**, 487 (2010); A. Maas, J. M. Pawlowski, D. Spielmann, A. Sternbeck, and L. von Smekal, Strong-coupling study of the Gribov ambiguity in lattice Landau gauge, Eur. Phys. J. C **68**, 183 (2010).

[55] A. Cucchieri and T. Mendes, Landau-gauge propagators in Yang-Mills theories at beta $= 0$: Massive solution versus conformal scaling, Phys. Rev. D **81**, 016005 (2010).

[56] A. Maas, Constructing non-perturbative gauges using correlation functions, Phys. Lett. B **689**, 107 (2010).

[57] A. Sternbeck and M. Müller-Preussker, Lattice evidence for the family of decoupling solutions of Landau gauge Yang-Mills theory, Phys. Lett. B **726**, 396 (2013).

[58] D. Dudal, M. S. Guimaraes, I. F. Justo, and S. P. Sorella, On bounds and boundary conditions in the continuum Landau gauge, Eur. Phys. J. C **75**, 83 (2015).

[59] C. S. Fischer and R. Alkofer, Infrared exponents and running coupling of SU(N) Yang-Mills theories, Phys. Lett. B **536**, 177 (2002).

[60] A. Sternbeck, E. M. Ilgenfritz, M. Muller-Preussker, A. Schiller, and I. L. Bogolubsky, Lattice study of the infrared behavior of QCD Green's functions in Landau gauge, *Proc. Sci.*, LAT2006 (2006) 076 [arXiv:hep-lat/0610053].

[61] M. Q. Huber and L. von Smekal, On the influence of three-point functions on the propagators of Landau gauge Yang-Mills theory, J. High Energy Phys. 04 (2013) 149; A. Blum, M. Q. Huber, M. Mitter, and L. von Smekal, Gluonic three-point correlations in pure Landau gauge QCD, Phys. Rev. D **89**, 061703 (2014); G. Eichmann, R. Williams, R. Alkofer, and M. Vujinovic, Three-gluon vertex in Landau gauge, Phys. Rev. D **89**, 105014 (2014).

[62] M. Haas, L. Fister, and J. M. Pawlowski, Gluon spectral functions and transport coefficients in Yang–Mills theory, Phys. Rev. D **90**, 091501 (2014); N. Christiansen, M. Haas, J. M. Pawlowski, and N. Strodthoff, Transport coefficients in Yang–Mills theory and QCD, arXiv:1411.7986.

[63] K. I. Aoki, M. Bando, T. Kugo, and M. G. Mitchard, Asymptotics of the pseudoscalar Bethe-Salpeter amplitude, Prog. Theor. Phys. **85**, 355 (1991).

[64] F. Buisseret, V. Mathieu, and C. Semay, Glueball phenomenology and the relativistic flux tube model, Phys. Rev. D **80**, 074021 (2009).

[65] D. Binosi, D. Ibanez, and J. Papavassiliou, Nonperturbative study of the four gluon vertex, J. High Energy Phys. 09 (2014) 059.

[66] A. K. Cyrol, M. Q. Huber, and L. von Smekal, A Dyson-Schwinger study of the four-gluon vertex, Eur. Phys. J. C **75**, 102 (2015).